

# PULSED RF CONTROL FOR THE P-LINAC TEST STAND AT FAIR\*

P. Nonn<sup>†</sup>, U. Bonnes, C. Burandt, F. Hug, M. Konrad,  
 N. Pietralla, Institut für Kernphysik, TU Darmstadt, Darmstadt, Germany  
 R. Eichhorn, Cornell University, Ithaca, NY, USA  
 W. Vinzenz, G. Schreiber, GSI, Darmstadt, Germany  
 H. Klingbeil, TEMF, TU Darmstadt, Darmstadt and GSI, Darmstadt, Germany

## Abstract

The p-Linac will be a dedicated proton injector for antiproton production at FAIR. It will provide a 70 MeV, 70 mA pulsed proton beam with a duty cycle of about  $10^{-4}$ . The RF of the normal conducting CH cavities will be pulsed, too. In order to test operation of these cavities a test stand is under construction at GSI. The RF control hardware and software for the test stand has been developed at TU Darmstadt. It is based on the digital low level RF control system used at the S-DALINAC. Hardware and software had to be customized in order to achieve pulsed operation within the given limits. These customizations along with measurements in pulsed operation will be presented.

## THE P-LINAC TEST-STAND AT FAIR

The Facility for Antiproton and Ion Research (FAIR) will be an international research infrastructure connected to the GSI Helmholtzzentrum für Schwerionenforschung (GSI) at Darmstadt, Germany. One of the main features of FAIR will be research using antiproton beams. In order to produce an antiproton beam that meets the needs of the experiments and the limitations of the beam transport, a pulsed proton beam of an energy of up to 70 MeV and a peak current of up to 70 mA is needed for injection into the SIS18 synchrotron. This proton beam will be provided by a dedicated linac, the p-Linac.

The main acceleration of the p-Linac will be provided by normal conducting, crossed-bar, h-mode (CH) cavities with a frequency of 325 MHz. These cavities will be driven by pulsed 2.5 MW klystrons [1]. These novel cavities and their peripheral devices have to be tested. Therefore an RF test stand is under construction at GSI, consisting of a bunker serving as radiation protection for the cavity and the klystron including a pulsed power supply, an isolator protecting the klystron and the necessary wave guides.

For this test stand a pulsed RF control system is needed, which achieves an amplitude stability of  $10^{-3}$  and a phase stability of  $0.1^\circ$ . It has been developed at TU Darmstadt, based upon the digital RF control system of the Superconducting Darmstadt Linear Electron Accelerator (S-DALINAC) [2].

\*Supported through BMBF contract no. 05P09RDRB5

<sup>†</sup>pnonn@ikp.tu-darmstadt.de

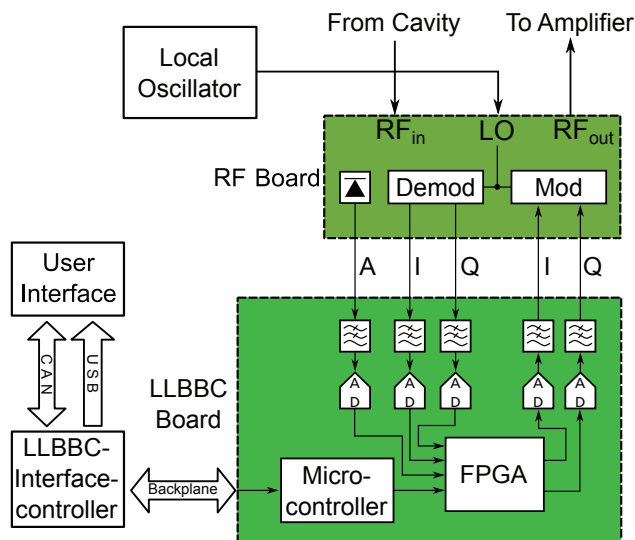


Figure 1: Diagrammatic overview of the low level baseband control system.

## THE S-DALINAC RF CONTROL SYSTEM

The control system for the superconducting and normal conducting cavities at the S-DALINAC operates at 3 GHz in cw mode [3]. As shown in fig. 1, it consists of two components, an RF board and a low level baseband control (LLBCC) board. The RF board (de)modulates the RF signals from/to baseband as an (I, Q) vector. An amplitude detector on the board provides the amplitude of the incoming RF signal. The LLBCC board processes the baseband signal from the RF board.

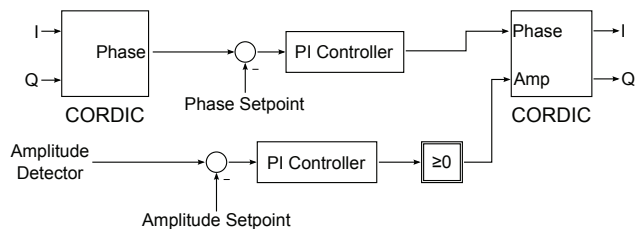


Figure 2: Flowchart of the control algorithm.

The controller is implemented as a repeating algorithm, which is executed by a custom made CPU. The latter is implemented in an FPGA while the algorithm is stored in

the memory of the FPGA and may be changed easily, even at runtime. The output of the control algorithm is fed to a digital to analogue converter (DAC) which provides the signal for the quadrature modulator on the RF board.

Figure 2 shows a flowchart representing the control algorithm for normal conducting cavities. The phase of the signal is computed from the  $(I, Q)$  vector using the CORDIC algorithm [4]. The amplitude is directly provided by the RF boards amplitude detector, in order to increase the accuracy. The amplitude and phase errors are calculated and fed to controllers. Both controllers are implemented as proportional-integral (PI) controllers. A second CORDIC algorithm computes the outgoing  $(I, Q)$  vector from the phase controller and amplitude controller outputs. See ref. [3] for further details.

## ADAPTIONS OF THE HARDWARE

### RF Board

Splitting the hardware into an RF board and a LLBBC board makes adaption to other frequencies easy [5]. As the quadrature (de)modulators of the S-DALINAC's RF boards cannot be used for frequencies below 400 MHz, a new RF board had to be designed. Tests have shown that these board provide a high accuracy [6].

### Filters

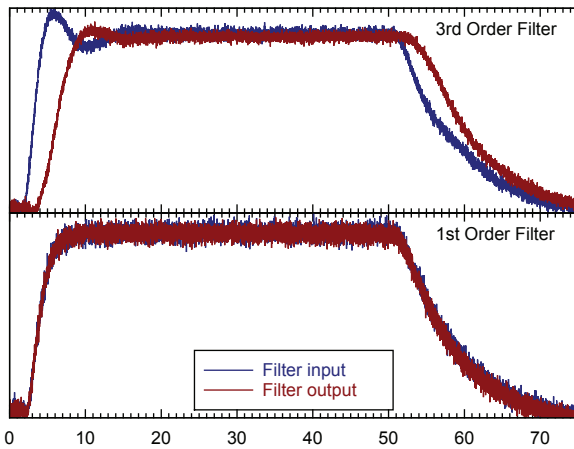


Figure 3: Signal transport through 3rd (top) and 1st order filter (bottom).

Low-pass filters are used in front of the ADCs and after the DACs (fig. 1). They serve as anti-aliasing and, for the DACs, as reconstruction filters. The filters for the superconducting 20 cell cavities of the S-DALINAC need an attenuation of -50 dB at 500 kHz in order to prevent the excitation of near pass-band modes. Thus 3rd order filters with an edge frequency of 100 kHz have to be used for the S-DALINAC. Figure 3 shows the latency of these filters.

As the next mode in the normal conducting CH cavities is about 900 kHz away [7], 3rd order filters are not needed

for the p-Linac. The filters have been reduced to 1st order filters with the same edge frequency, still providing an attenuation of about -24 dB at 500 kHz. Figure 3 shows that the latency is reduced, improving the rise-time of the control system.

## ADAPTIONS OF THE CONTROL ALGORITHM

### Pulsed Amplitude Control

A time-dependent amplitude setpoint is one of the first adaptations needed for pulsed operation. It has been implemented as an addressed list of setpoints. Its reading address is incremented every time the control loop restarts. This list, called PMEM, holds one amplitude setpoint for every iteration of the control algorithm and thus is capable of generating arbitrary pulse shapes.

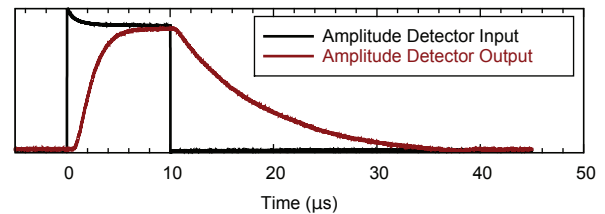


Figure 4: Measured pulse response of the amplitude detector.

### Amplitude Detection

The hardware amplitude detector shows an insufficient response time (see fig. 4). To improve the rise-time of the control system the amplitude has to be computed from the  $(I, Q)$  vector. The first CORDIC algorithm has been reconfigured to provide an amplitude output. For timing reasons it became impossible to provide the amplitude controller output to the second CORDIC. This was solved by using the output of the amplitude controller to scale the  $I$  and  $Q$  outputs of the second CORDIC.

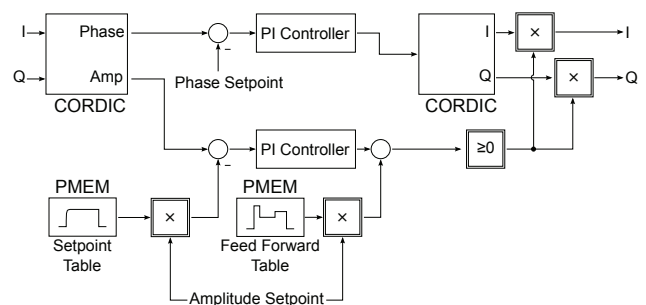


Figure 5: Flowchart of the control algorithm for pulsed operation.

### Feed Forward

To improve the response time further a feed forward control has been implemented. This has been done by gener-

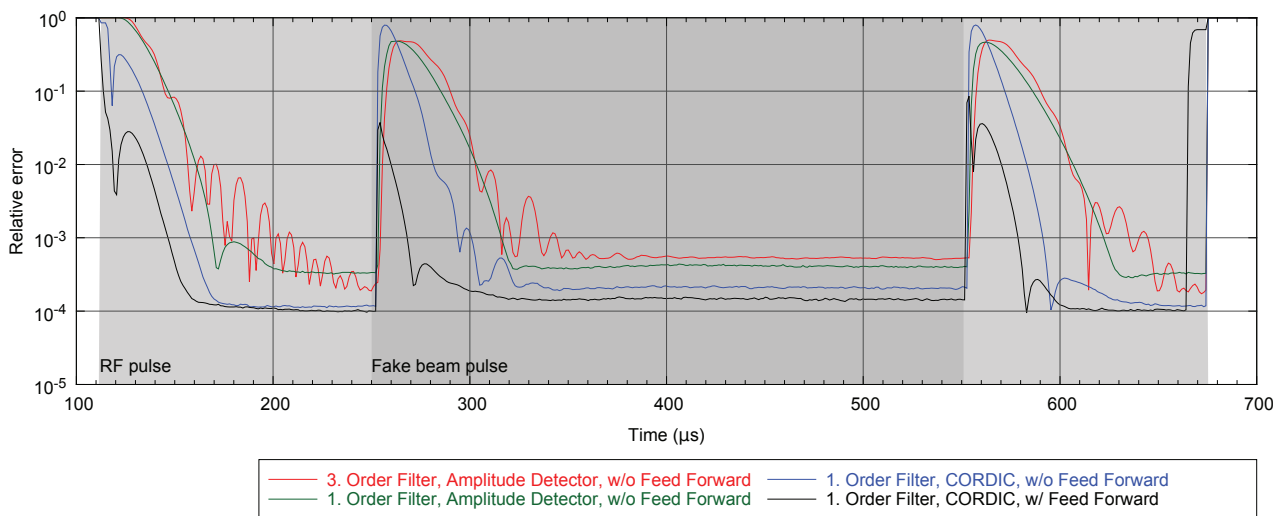


Figure 6: Root mean square amplitude errors of a pulsed cavity with simulated beam loading for different control system setups.

ating a second instance of PMEM and adding its output to the output of the amplitude controller.

Figure 5 shows a flowchart of the pulsed control algorithm using feed forward and the fast CORDIC-based amplitude detection. Also a common scaling factor for amplitude setpoint and feed forward has been implemented. This allows scaling of the pulse shape without the need to change both PMEMs.

**MEASUREMENTS**

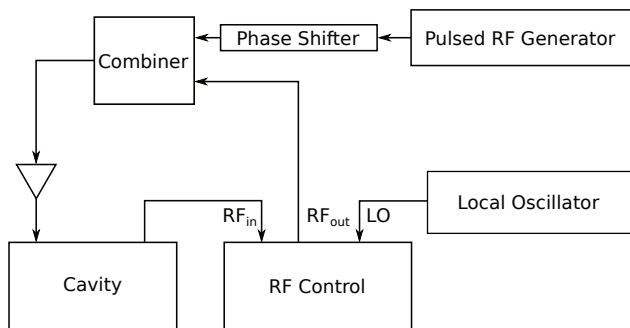


Figure 7: Scheme of the test setup.

In order to study the impact of the improvements, a series of measurements was performed. Figure 7 shows a schematic overview of the setup used for the measurements. To simulate beam loading, a pulsed RF signal shifted by 180° was combined with the RF output of the control system.

Figure 6 shows the relative amplitude errors over a pulse for different implementations of the control system. Every graph represents the root mean square of about 2000 pulses. The graphs show how the time needed to draw the relative error below 10<sup>-3</sup> decreases with every further change of the

control system. The response time to beam loading has been reduced from about 100 μs to about 20 μs. The response time may be lowered further by refinement of the feed-forward pulse shape.

**SUMMARY**

The RF control system of the S-DALINAC has been successfully adapted for pulsed operation at 325 MHz. An RF board for lower frequencies, including 325 MHz, has been designed and tested. Both RF boards together cover the frequency range from 50 MHz to 6 GHz. Filters, amplitude detection and control algorithm have been modified to improve the response time of the control system to match the needs of the p-Linac at FAIR. Measurements have shown the response time improvements of these measures.

**REFERENCES**

- [1] "FAIR - Baseline Technical Report", 2006, Volume 2, p. 335-339
- [2] A. Richter, "Operational Experience at the S-DALINAC, 1996, EPAC'96, Sitges, p. 110
- [3] M. Konrad et al., "Digital base-band rf control system for the superconducting Darmstadt electron linear accelerator", Phys. Rev. ST Accel. Beams 15, 052802 (2012)
- [4] Xilinx, "Datasheet: LogiCORE IP CORDIC v5.0", [http://www.xilinx.com/support/documentation/ip\\_documentation/cordic/v5\\_0/ds858\\_cordic.pdf](http://www.xilinx.com/support/documentation/ip_documentation/cordic/v5_0/ds858_cordic.pdf)
- [5] A. Araz et al., "The Low Level Base Band RF Control for the S-DALINAC: A Flexible Solution for Other Frequencies?", SRF 2009, Berlin, THPPO048, p. 689
- [6] M. Konrad et al., "Development of a Digital Low-Level RF Control System for the p-Linac Test Stand at FAIR", IPAC'12, New Orleans, THPPC075, p. 3461
- [7] R. Brodhage et al., "First Measurements of an Coupled CH Power Cavity for the FAIR Proton Injector", IPAC'12, New Orleans, THPPP036, p. 3812